SHP-2 deletion in postmigratory neural crest cells results in impaired cardiac sympathetic innervation

Jacquelyn D. Lajiness[a], Paige Snider[a], Jian Wang[a], Gen-Sheng Feng[b], Maike Krenz[c], and Simon J. Conway[a,1]

[a]Developmental Biology and Neonatal Medicine Program, Herman B Wells Center for Pediatric Research, Indiana University School of Medicine, Indianapolis, IN 46202; [b]Department of Pathology, and Division of Biological Sciences, University of California, San Diego, La Jolla, CA 92093; and [c]Department of Medical Pharmacology and Physiology, Dalton Cardiovascular Research Center, University of Missouri Columbia, Columbia, MO 65211

Edited by Marianne E. Bronner, California Institute of Technology, Pasadena, CA, and accepted by the Editorial Board February 19, 2014 (received for review October 14, 2013)

Autonomic innervation is an essential component of cardiovascular regulation that is first established from the neural crest (NC) lineage in utero and continues developing postnatally. Although in vitro studies have indicated that SH2-containing protein tyrosine phosphatase 2 (SHP-2) is a signaling factor critical for regulating sympathetic neuron differentiation, this has yet to be shown in the complex in vivo environment of cardiac autonomic innervation. Targeting SHP-2 within postmigratory NC lineages resulted in a fully penetrant mouse model of diminished sympathetic cardiac innervation and concomitant bradycardia. Immunohistochemistry of the sympathetic nerve marker tyrosine hydroxylase revealed a progressive loss of adrenergic ganglionic neurons and reduction of cardiac sympathetic axon density in *Shp2* cKOs. Molecularly, *Shp2* cKOs exhibit lineage-specific suppression of activated phospo-ERK1/2 signaling but not of other downstream targets of SHP-2 such as pAKT. Genetic restoration of the phosphorylated-extracellular signal-regulated kinase (pERK) deficiency via lineage-specific expression of constitutively active MEK1 was sufficient to rescue the sympathetic innervation deficit and its physiological consequences. These data indicate that SHP-2 signaling specifically through pERK in postmigratory NC lineages is essential for development and maintenance of sympathetic cardiac innervation postnatally.

birth defects | conditional mouse knockout | heartbeat | Shp2-pERK | sympathetic neural crest

Although autonomic innervation of the heart begins in utero, functional neurocardiac coupling continues postnatally. Autonomic imbalance and irregular cardiac innervation density result in deadly consequences such as cardiac arrhythmias, heart failure, and sudden cardiac death (1–4). Although a balance between the sympathetic and parasympathetic arms of the autonomic nervous system is required to regulate heart rate, conduction velocity, and the force of each contraction, sympathetic tone predominates in determining the basal heart rate in the mouse.

The sympathetic nervous system arises from the neural crest (NC) lineage. Trunk NC cells delaminate and migrate ventrally through the somites to establish the sympathetic trunk ganglia near the dorsal aorta (5, 6). Postmigration, cross-regulatory transcription factors such as Mash1, Phox2a and 2b, and Gata3 (7–13) are temporarily expressed and drive these NC cells to acquire a neuronal fate and eventually to differentiate into sympathetic neurons expressing both neuron specific β-tubulin (NSβT) and tyrosine hydroxylase (TH; the rate-limiting enzyme in catecholamine synthesis) (14–19). From there, a subset of sympathetic NC cells undergoes a second migration to the cervicothoracic and intrinsic cardiac ganglia to establish populations of sympathetic neurons which contribute to the cardiac plexus or "heart brain" (5, 20, 21). Recent studies exploring the extensive complexity of autonomic cardiac innervation revealed multiple levels of regulation and interaction between parasympathetic and sympathetic arms of autonomic innervation that converges in the heart brain to control cardiac function (20–26). Sympathetic (i.e., TH-positive) innervation is first observed at the base of the fetal heart; this innervation then extends onto the surface of the atria and eventually to the ventricles before following blood vessels into the ventricular wall to innervate the myocardium and project to the sinoatrial and atrioventricular nodes postnatally (27). The sympathetic innervation of the heart is not functionally relevant (i.e., does not control heart rate) until the second postnatal week of life in rodents (23, 28, 29), and the adult pattern of innervation is not fully achieved until 3 wk after birth (23, 30). This developmental process requires nerve growth factor (NGF), which is produced by the target organ (the myocardium in the case of the heart) and is the main neurotrophic factor in establishing and maintaining sympathetic innervation (31). In vitro studies have shown that NGF stimulates the differentiation/neurite outgrowth of sympathetic neurons through the SHP-2 (*Src homology protein-tyrosine phosphatase 2*)/ERK pathway while mediating the survival of those same neurons through the PI3K/AKT pathway (32–34). Interruption of the NGF signaling pathway at either the ligand (NGF) or receptor (TrkA) level results in pups that are viable at birth without any gross defects; however, the pups fail to gain weight, have smaller ganglia and fewer dendrites, exhibit total loss of sympathetic innervation by 10 d after birth, and die ∼4 wk (*Ngf* null) or ∼8 wk after birth (*TrkA null*) (35–38). Other models of altered sympathetic innervation including a *p75* null (a low-affinity receptor of NGF) as well as systemic loss of *Sema3a* (a neural chemorepellent for sensory and sympathetic axons) and NC-restricted deletion of the SEMA3A receptor *Nrp1* all result in diminished sympathetic innervation and subsequent bradycardia (24, 39, 40).

SHP-2 is a ubiquitously expressed nonreceptor tyrosine phosphatase involved in a variety of cellular functions including

Significance

Initial heart development takes place independently of its innervation; however, impaired postnatal cardiac sympathetic innervation can result in deadly consequences. This study provides evidence that the signaling molecules SHP-2 and phosphorylated-extracellular signal-regulated kinase (pERK) are critical components in the development of cardiac sympathetic innervation. Interruption of this signaling cascade resulted in decreased sympathetic innervation and decreased heart rate. Genetic rescue of downstream pERK signaling restored both cardiac innervation and heart rate. Thus, this work lends mechanistic insight into clinical presentations of diseases associated with alterations in this signaling pathway such as LEOPARD syndrome as well as other ECG abnormalities resulting from disturbed pERK-dependent sympathetic innervation.

Author contributions: S.J.C. designed research; J.D.L., P.S., J.W., and S.J.C. performed research; G.-S.F. and M.K. contributed new reagents/analytic tools; J.D.L., P.S., and S.J.C. analyzed data; and J.D.L. and S.J.C. wrote the paper.

The authors declare no conflict of interest.

This article is a PNAS Direct Submission. M.E.B. is a guest editor invited by the Editorial Board.

[1]To whom correspondence should be addressed. E-mail: siconway@iu.edu.

This article contains supporting information online at www.pnas.org/lookup/suppl/doi:10.1073/pnas.1319208111/-/DCSupplemental.

survival, proliferation, and differentiation (41–45). Significantly, mutations in SHP-2 (encoded by PTPN11) result in LEOPARD syndrome (LS; OMIM 151100), which is part of a family of autosomal dominant syndromes termed "RASopathies" (46). There are seven SHP-2 mutations associated with LS, all of which are concentrated in the catalytic core of the protein. These mutations have been shown in vitro to cause a decrease in catalytic activity of SHP-2 and diminished MAPK signaling (42, 47, 48); however, there is still debate as to the mechanism for how SHP-2 facilitates Ras/MAPK activation. It has been hypothesized that SHP-2 dephosphorylates binding sites on Ras GAP receptors, inactivates Grb2/Sos inhibitors, and activates Src family kinases resulting in sustained Ras and subsequent ERK activation (42, 49, 50). LS itself is characterized by a constellation of symptoms such as heart defects and electrocardiographic (ECG) abnormalities including sinus bradycardia, although the ECG anomalies observed are often complicated by structural defects (51, 52).

Due to its pivotal developmental role, systemic *Shp2* deletion results in early embryonic lethality (53, 54); however, several conditional knockout (cKO) mouse models have investigated the embryonic in vivo requirement of SHP-2 using various Cre recombinase drivers. These models, although primarily embryonically lethal, have demonstrated that SHP-2 can play a role in NC-mediated events such as cardiac outflow track development, semilunar valvulogenesis (55), and Schwann cell-mediated myelination of the peripheral nervous system (41, 56). Additional in vitro studies have shown that SHP-2 is a key downstream factor in NGF signaling during sympathetic neuronal differentiation and subsequent neurite outgrowth (57–59), but the in vivo postnatal requirement of SHP-2 within postmigratory NC lineage has remained unclear.

In the present study, we sought to explore the in vivo postnatal role of SHP-2 and its downstream effectors within the development and maintenance of cardiac sympathetic innervation and neurocardiac coupling. We targeted SHP-2 using a *Postn-Cre* transgenic line that expresses Cre within postmigratory NC lineages (60). The mutants exhibit failed sympathetic cardiac innervation and concomitant bradycardia. Molecular analysis indicated suppression of phosphorylated-extracellular signal-regulated kinase (pERK) signaling within the sympathetic lineage. Further investigation revealed that genetic restoration of ERK signaling via lineage-specific expression of constitutively active mitogen-activated protein kinase kinase-1 (caMEK1) was sufficient to rescue the sympathetic innervation deficit and its physiological consequences. These results demonstrate that SHP-2 promotion of the ERK pathway is required in vivo for establishment of functional sympathetic innervation within the postnatal heart. Moreover, these data provide a mechanistic basis for understanding the lineage-specific aspects of clinical presentations that can occur in diseases such as LEOPARD syndrome as well as other ECG abnormalities resulting from disturbed pERK-dependent sympathetic innervation.

Results

***Shp2* cKOs Are Indistinguishable from Control Littermates at Birth.** Conditional *Shp2* floxed mice containing a floxed exon 4 (50) were intercrossed with *Postn-Cre* transgenic mice to generate embryos that were deficient for SHP-2 protein within many postmigratory NC lineages. *Postn-Cre* mice express Cre under the control of a partial 3.9 kb *Periostin* promoter [as demonstrated by *R26r* indicator mice (61)] within the E11.5 and older peripheral nervous system (including autonomic, sensory, and enteric components), as well as the endocardial cushion lineages and future valves from embryonic (E) day 10 onward, but is absent from the CNS (60, 62) (Fig. 1 *A–E*). *Postn-Cre* is also expressed in fetal and neonatal cardiac fibroblasts (63) but is absent from in utero and postnatal cardiomyocytes (63, 64).

Homozygous *Shp2* cKO newborns were genotyped via PCR at expected Mendelian inheritance ratios ($n = 11$ litters) and lineage mapping using the *R26r* reporter (61) confirmed Cre-mediated recombination in a pattern suggestive of postmigratory NC lineages from E11.5 onward (Fig. 1 *A–E*). This demonstrated that our conditional gene-targeting strategy did disrupt normal SHP-2 expression in utero but did not cause any gross embryonic defects and circumvented the in utero lethality observed within other NC-restricted models of SHP-2 ablation (43, 53). *Shp2* cKOs were indistinguishable from littermate controls at birth (Fig. 1*F*), but by the second week of life, 100% of the mutants exhibited diminished growth ($n = 74/74$ cKOs), and none survived past postnatal (P) day 21. Because a previously reported *Shp2* cKO model using *Nestin-Cre* exhibited a more severe phenotype in males (65), we used PCR analysis [using *Zfy* sex determination primers (66)] to determine sex of all neonatal mutants; however, we did not detect any sex-related bias in our model ($n = 24$ cKOs). Necropsy verified normal craniofacial and cardiovascular development. Similarly, histology and *R26r* reporter analysis revealed that despite Cre expression within the embryonic outflow tract and valves, both outflow tract morphogenesis and valvular maturation were unaffected; however, diminished peripheral and enteric innervation were noted and are most likely contributing factors to the eventual lethality observed (*SI Appendix*, Fig. S1). Lineage-specific recombination was verified in DNA isolated from mutant sympathetic trunk ganglia (Cre-expressing) but not brain (Cre-negative as indicated by *lacZ* expression for all ages of interest in this study) (Fig. 1*G*). Deletion of exon 4 of *Shp2* resulted in decreased SHP-2 protein levels in microdissected partial heart/cardiac ganglia samples (Fig. 1*H*) and NC-containing adrenals (*SI Appendix*, Fig. S2). These tissues were chosen because they are enriched for *Postn-Cre*–expressing cells (Fig. 1 *A–E*); however, it is important to remember that neither the partial heart/cardiac ganglia nor the adrenal gland is entirely Cre-positive so it is unlikely that ubiquitous SHP-2 would be completely eliminated in these samples.

Postnatally, *Shp2* cKOs Exhibit Diminished Neurite Outgrowth from Cardiac Sympathetic Ganglia. To investigate the NC-specific effects of *Shp2* KO in postmigratory NC lineages, we carried out *R26r* lineage mapping using the *lacZ* reporter system (61). The largest component of sympathetic innervation projects to the dorsal surface of the heart, and there, we observed significantly diminished neurite outgrowth from cKO TH-positive cardiac ganglia at both P2 and P14 (Fig. 1 *I–T*). Whole-mount *lacZ* spatiotemporal analysis revealed that mutant cardiac sympathetic ganglia have fewer projections and that the neurites that are present are less robust (Fig. 1 *I*, *J*, *O*, and *P*) than those observed in age-matched littermate controls (Fig. 1 *L*, *M*, *R*, and *S*). The cKO ganglia themselves, however, do not appear grossly atrophic or morphologically compromised. Detailed histology revealed typical neuronal architecture, namely, large dense nucleus with wavy axonal projections emanating from both the control (Fig. 1 *N* and *T*) and the cKO ganglia (Fig. 1 *K* and *Q*).

Decreased Sympathetic Innervation Is Observed in cKO Hearts. In light of the decreased neurite outgrowth despite the normal gross anatomical appearance of the ganglia, molecular characterization of cKO cardiac ganglia using immunohistochemistry techniques was conducted. Despite the in utero loss of SHP-2, E14.5 cKO ganglia consistently express neuron-specific NSβT, TrkA (the high-affinity receptor of NGF, required for sympathetic neuron survival), and the sympathetic neuronal marker TH (Fig. 2 *A–C*). A similar pattern was observed in E16.5 cKO ganglia (*SI Appendix*, Fig. S3). However, postnatally, the expression of TH in mutant ganglia is diminished at all ages investigated [P7 (Fig. 2*F*) and P0, P6, and P18 (*SI Appendix*, Fig. S3)], whereas NSβT and TrkA remain unaltered (Fig. 2 *D* and *E*). Moreover, the postnatal

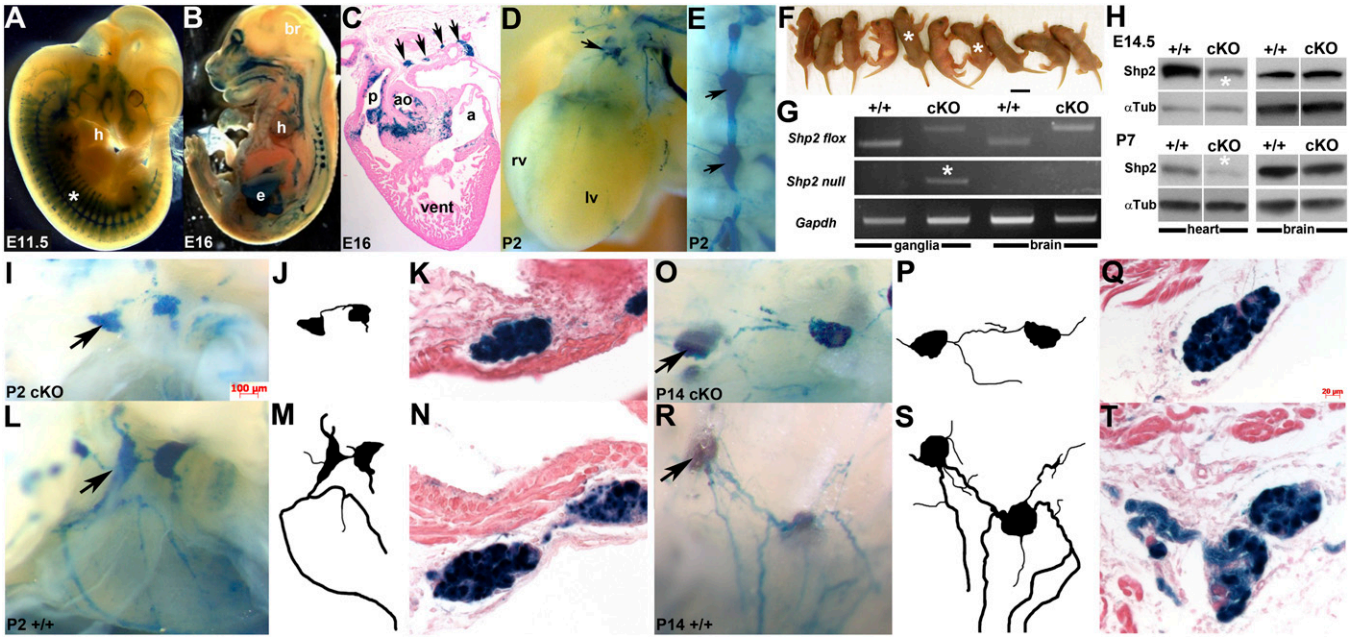

Fig. 1. *Shp2* cKOs exhibit diminished neurite outgrowth from cardiac sympathetic ganglia. (*A–E*) Lineage mapping of *Postn-Cre* expression via *lacZ* staining of E11.5 embryo (*A*), E16 embryo (*B* and *C*), and P2 pup (*D* and *E*) demonstrated Cre expression pattern suggestive of postmigratory NC lineages including the craniofacial region, dorsal root ganglia, sympathetic trunk (* in *A*, *B*, and *E*), enteric ganglia, and peripheral nerves including those innervating the heart (*A–D*; arrows in *C*). (*F*) Litter of P2 pups (mutants indicated by *) demonstrating *Shp2;Postn-Cre* cKOs are indistinguishable from littermate controls. (*G*) PCR analysis of recombination efficiency demonstrating the lineage-specific nature of *SHP-2* KO. Recombination efficiency was calculated via densitometry to be 78.8% within cKO ganglia (*). (*H*) Composite Western blot of heart and brain isolates confirming the lineage-specific nature of *Shp2* cKO at the protein level. SHP-2 levels were decreased in heart (*) but not brain isolates both in utero and postnatally. (*I–K*) P2 mutant TH-positive cardiac ganglia (arrows): whole-mount *lacZ* staining (*I*), black and white reconstruction trace of surface neurite outgrowth (*J*), and histological section of *lacZ* stained ganglia counterstained with eosin (*K*). (*L–N*) Same sequence of littermate P2 control. (*O–T*) Same sequence of P14 mutant (*O–Q*) and littermate P14 control (*R–T*). Note that both P2 and P14 cKOs exhibit reduced neurite outgrowth. [Scale bars: 100 μm (*I*, *L*, *O*, and *R*) and 20 μm (*K*, *N*, *Q*, and *T*).]

cKO ganglia are similar in size and cellularity to controls, and TUNEL staining did not detect any apoptotic cells (Fig. 2*G*). Radioactive in situ revealed mutant ganglia aberrantly express markers of early embryonic sympathetic neuronal differentiation because both *Phox2a* and *Phox2b* mRNA were expressed in mutant but not control ganglia (Fig. 2 *I–N*). Additional embryonically expressed sympathetic neuronal differentiation factors (*Gata3, Sox10,* and *Mash1*) were also investigated but were found to be negative in both controls and mutants. Significantly, global cardiac sympathetic innervation of the cKO was compromised. At day 0, nodules of TH-positive innervation can be observed in control (arrows in Fig. 2*O*) but not mutant hearts (Fig. 2*P*), and by P7 the mutant has substantially decreased TH-positive innervation (Fig. 2 *Q* and *R*), particularly around the blood vessels supplying the ventricles (where sympathetic innervation is most pronounced in the control). Diminished TH-positive innervation was also observed in E16.5, P6, and P18 cKO hearts (*SI Appendix*, Fig. S3). Despite diminished global cardiac sympathetic innervation, the epicardial-to-endocardial gradient was present in controls and mutants (*SI Appendix*, Fig. S3 *I–L*).To further validate diminished TH expression in cKOs, Western analysis performed on isolated hearts confirmed that TH levels were decreased by 70% in mutants versus controls (Fig. 2*H*).

***Shp2* cKOs Experience Sinus Bradycardia.** To investigate whether the observed SHP-2–dependent innervation defect has any functional impact, longitudinal ECG analysis was carried out from P4 to P20. These studies revealed that cKOs exhibit sinus bradycardia (two-way ANOVA, $P = 0.0012$; Fig. 3 *A* and *B*) beginning at P12, corresponding to the developmental timing of sympathetic control of heart rate (28, 29). At P6, before the sympathetic nervous system is thought to be functionally relevant for establishing basal heart rate, there is no difference between mutants and littermate controls (Fig. 3 *A* and *B*). However, by P12 the heart rates of the control pups significantly increased (this increase is associated with establishment of sympathetic control of heart rate), whereas the cKO heart rate showed no corresponding increase (Fig. 3 *A* and *B*). By P17 the heart rates of the control littermates have plateaued, whereas the cKO heart rates continue to decrease until lethality at 3 wk of age (Fig. 3 *A* and *B*). No other arrhythmias or anomalies in the ECG wave form (P-wave duration, PR, or QRS intervals) were observed throughout the study with the exception of mild prolongation of the PR interval immediately preceding death (*SI Appendix*, Table S1). However, the first-degree heart block never progressed and may be complicated by other issues such as the weight loss that was observed in the final 24 h of life. QT intervals were also examined, but the absence of a definitive T wave in many traces negated the utility of such an investigation.

To examine the underlying cause of the sinus bradycardia, several pharmacological interventions were used. Due to the diminished sympathetic innervation observed in the cKO heart (see Fig. 2), we hypothesized that the lack of adrenergic stimulation was directly responsible for the observed phenotype. To test this, we directly activated the β-adrenergic receptors (the receptors that would normally be stimulated by sympathetic neuron release of norepinephrine) by administering an i.p. injection of the β-adrenoreceptor agonist, isoproterenol. Isoproterenol increased the heart rates of both the control and mutant by 30% with respect to their basal heart rates (Fig. 3*C*). Moreover, the relative increase is consistent with the results reported from isoproterenol challenge tests carried out in adult mice (67) and confirms that the cKO cardiomyocytes are capable of responding to adrenergic stimulation. In contrast, inhibiting parasympathetic

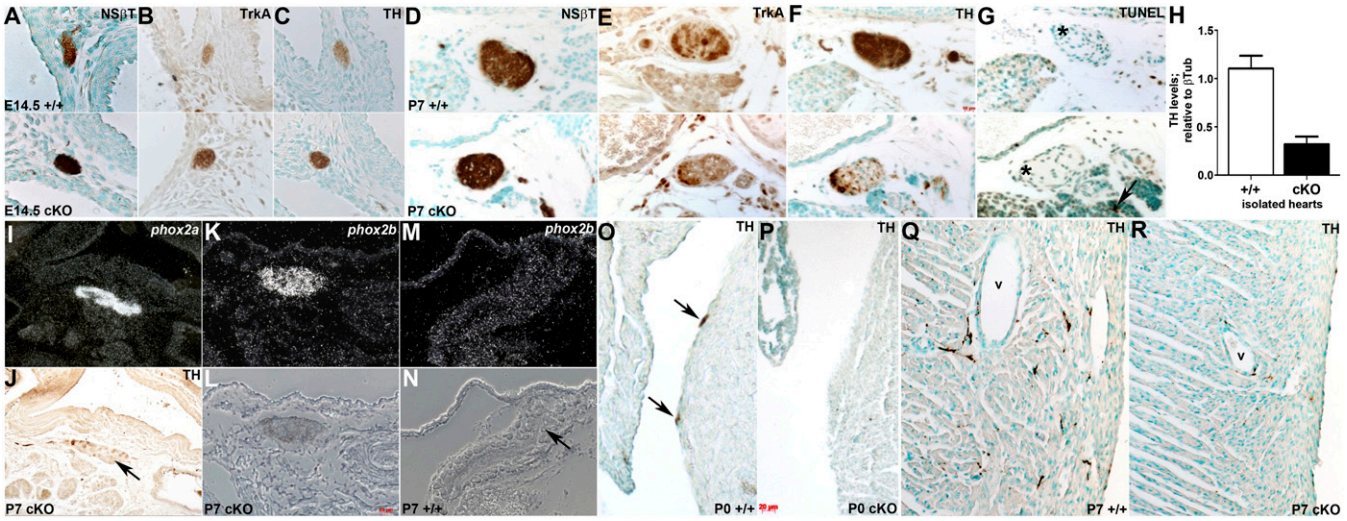

Fig. 2. *Shp2* cKOs demonstrate diminished cardiac sympathetic innervation. (*A*–*C*) Immunohistochemistry (IHC) demonstrating equivalent NSβT (*A*), the NGF receptor TrkA (*B*), and TH (*C*) expression in E14.5 littermate pairs of controls (*Upper*) and mutant (*Lower*) ganglia. (*D*–*G*) Adjacent sections of P7 ganglia examined using IHC NSβT (*D*), TrkA (*E*), TH (*F*), and apoptosis (TUNEL; *G*). Note that P7 cKO ganglia exhibited diminished TH expression but are not apoptotic. However, apoptotic cells are seen in adjacent tissue (arrow in cKO in *G*; $n = 3$ littermate pairs with two slides containing four to five sections of tissue each analyzed). (*H*) Densitometry quantification of TH protein levels as detected by Western within isolated P14 hearts ($n = 5$). cKO TH levels were significantly decreased (*t* test; *P* value = 0.0010). (*I* and *J*) In situ hybridization of mutant cardiac ganglia showing aberrant expression of *Phox2a* (an embryonic sympathetic neuronal differentiation marker; *I*) in the context of diminished TH expression (arrow in *J*). (*K* and *L*) In situ hybridization of mutant cardiac ganglia showing aberrant expression of *Phox2b* (an embryonic sympathetic neuronal differentiation marker; *K*). *L* shows phase contrast of the ganglia itself. (*M* and *N*) Representative in situ hybridization of control cardiac ganglia showing no expression of *Phox2b* (*M*). *N* is phase contrast of the ganglia. (*O* and *P*) IHC detection of TH-positive nerves on the left ventricle of a P0 control (*O*) and mutant (*P*). (*Q* and *R*) TH IHC of P7 ventricle of a control (*Q*) and mutant (*R*). Note the lack of sympathetic innervation in the mutant heart at both ages but normal surface (arrows in *O*) and penetrating (*Q*) TH-positive nerves around blood vessel (v) in wild types. Error bars represent SEM.

activity with atropine had no significant effect on either mutants or controls (*SI Appendix*, Fig. S4*C*). This was not particularly surprising due to the fact that the parasympathetic influence on murine heart rate is often minimal and subject to change on differing genetic backgrounds (68, 69). To exclude the possibility that the β-adrenergic receptors or their downstream signaling effectors were misexpressed, we performed qPCR for both the *β1-adrenergic receptor* (the primary adrenergic receptor expressed in the heart) and *adenylate cyclase-6* (the enzyme that produces cAMP as a second messenger to propagate the adrenergic signal). Levels of both targets were found to be normally expressed in P14 cKO hearts (*SI Appendix*, Fig. S4). Furthermore, heart *Ngf* levels (as quantified via qPCR) were found to be the same between mutant and control for all ages investigated (Fig. 3*D*). This was expected because regulation of NGF synthesis throughout development is independent of sympathetic innervation or norepinephrine secretion at the target organ (70), suggesting that the diminished cardiac innervation does not affect the induction of neurotrophic factors within the cKO heart.

To rule out any potential abnormalities in the sinoatrial node (SAN) as possible contributing factors to the sinus bradycardia observed, *Hcn4* expression was examined. HCN4 is a key channel located primarily in the SAN that helps maintain a regular heart rhythm. Significantly, no disparities between control and mutant SANs were observed (*SI Appendix*, Fig. S5 *A*–*D*). Also, because *Postn-Cre* is expressed in cardiac fibroblasts which are responsible for insulating the intrinsic conduction system of the heart, *lacZ*-positive fibroblasts were quantified and found to be comparable between mutants and controls at all ages investigated. Additionally, the levels of αSmooth muscle actin (a marker robustly expressed by cardiac fibroblasts) were equitable, indicating that cKO cardiac fibroblasts are present, are appropriately localized, and express normal markers (*SI Appendix*, Fig. S5 *E*–*H*). Although histology did not reveal any structural abnormalities, the microstructures of the control and mutant ventricular myocardium were further investigated via electron microscopy. Similar to the histological, lineage mapping, and qPCR data above, the contractile apparatus and mitochondrial architecture were not found to differ between mutant and control (Fig. 3 *E* and *F*), indicating that *Postn-Cre*–mediated lineage-restricted loss of SHP-2 does not adversely affect the cKO heart itself.

Decreased pERK Is a Primary Signaling Abnormality Observed in Mutants. SHP-2 is an important factor in several signaling cascades, particularly modulation of the MAPK cascades (49). Published data have shown that cKO of SHP-2 within premigratory NC results in diminished pERK signaling and that transient ERK1/2 activation is necessary for expression of smooth muscle and neural markers in NC in vitro (53). Similarly, SHP-2–deficent hematopoietic stem and progenitor cells show defective ERK and AKT activation (71). In contrast, SHP-2–impaired cardiomyoctes exhibit increased levels of phosphorylated AKT (pAKT) (72–74). Because they are the two major postnatal effector molecules studied in models of SHP-2 dysregulation, we examined pERK and pAKT levels. Western analysis of microdissected heart/cardiac ganglia protein isolates (containing only the top of the hearts/atria that are enriched for Cre-positive cells) revealed that pERK levels were decreased in cKOs by 50% at both E14.5 and P7 (Fig. 4). However, cKO pAKT levels were unaltered both in utero and postnatally. These results indicate that the ERK1/2 branch of the MAPK pathway as opposed to the AKT pathway is selectively affected in the *Shp2;Postn-Cre* mutants and suggest that SHP-2 activity in the postmigratory NC is essential for pERK-mediated differentiation and establishment of cardiac sympathetic neurons but not their survival, which is dependent on AKT signaling.

Genetic Restoration of pERK Signaling Rescues the Cardiac Innervation Defect. We next determined whether diminished pERK levels were directly responsible for the sympathetic innervation phenotype observed in *Shp2* cKOs. To reactivate ERK1/2 signaling, a conditional

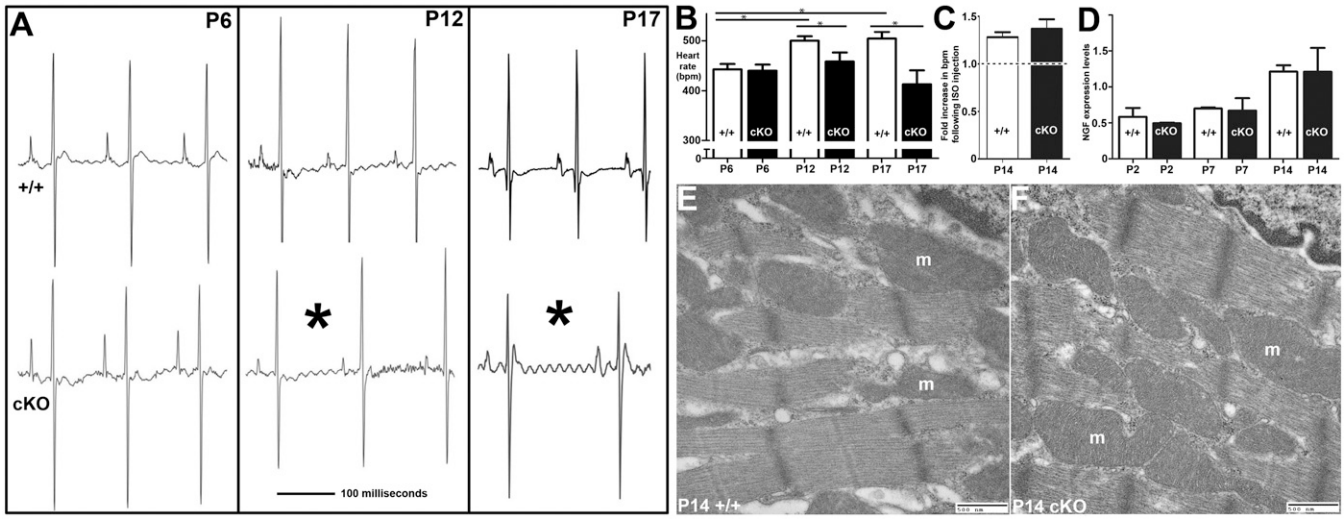

Fig. 3. SHP-2 mutants exhibit progressive sinus bradycardia that is reversible by administration of a β-adrenergic agonist. (*A*) Characteristic ECG traces from a wild-type littermate control (*Upper*) and a *Shp2 cKO* mutant (*Lower*) at three different ages [P6, before sympathetic innervation is functionally relevant to heart rate; P12, once sympathetic innervation is functionally established; and P17, demonstrating the continual decline of mutant heart rate (indicated via *)] are shown. (*B*) Graphic representation of average heart rates collected at the three ages in *A*. The heart rate of control animals increased from P6 to P12 and then plateaued, whereas the cKO heart rate never significantly changed [two-way ANOVA, Sidak's multiple comparisons $^{+/+}$: P6 vs. P12, $P < 0.05$; P6 vs. P17, $p < 0.05$; P12 vs. 17 = nonsignificant ($P > 0.05$); mutant: none of the comparisons of different time points were significant; control vs. mutant: P6, nonsignificant; P12, $P < 0.05$; P17, $P < 0.05$ ($n = 7$–19)]. (*C*) Graphic representation of heart rate increase (normalized to basal heart rate, indicated by dotted line) following i.p. injection of isoproterenol (2 mg/kg body weight). Both mutant and control heart rates increased with isoproterenol administration (paired *t* test; $P = 0.003$); however, the genotype of the animal did not affect the degree to which the heart rate was elevated [two-way ANOVA interaction (genotype x treatment): $P = 0.905$ ($n = 4$–6)]. (*D*) qPCR analysis illustrating comparable levels of *Ngf* between control and mutant hearts throughout the first 2 wk of life. (*E* and *F*) Electron microscopy examination of control and mutant myocardium revealed normal contractile apparatus and mitochondrial (m) architecture in the P14 mutant and control hearts. (Scale bar: 500 nm.) Error bars represent SEM.

floxed-stop model of *caMEK1* (the effector directly upstream of ERK) was crossed onto the *Shp2;Postn-Cre* background (Fig. 5*A*). In this model, any cell expressing Cre will simultaneously delete SHP-2 and express caMEK1 (75) in a lineage-restricted manner. The *Shp2;Postn-Cre;caMEK* mice had significantly higher pERK levels than their non-caMEK1–expressing mutant littermates, and the *Shp2;Postn-Cre;caMEK* pERK levels were comparable to wild-type age-matched littermate controls (Fig. 5*B*). *Shp2;Postn-Cre;caMEK* TH levels were similarly restored to wild-type levels (Fig. 5*C*). Moreover, immunohistochemistry revealed restoration of TH expression throughout the *Shp2;Postn-Cre;caMEK* cardiac ganglia (Fig. 5 *D–F*) and an increase in TH-positive innervation properly localized around the blood vessels in the myocardium of the *caMEK1*-expressing cKO ventricle (Fig. 5 *G–I*). The restored sympathetic innervation on the dorsal surface of the P14 *Shp2;Postn-Cre;caMEK* heart was verified via whole-mount TH-immunostaining. This revealed substantially increased arborization in the "rescued" mutant compared with the non-rescued *Shp2;Postn-Cre* mutant (Fig. 5 *J–L*). Consequently, heart rates of *Shp2;Postn-Cre;caMEK* rescued mutants were found to be normalized to control levels at all ages investigated (P14 shown; Fig. 5*M*). Thus, the rescue of sympathetic innervation functionally

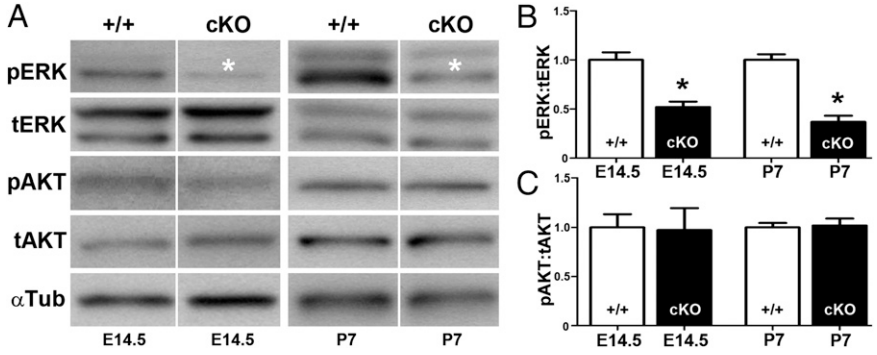

Fig. 4. *Shp2* cKOs exhibit decrease in cardiac pERK signaling both embryonically and postnatally, whereas pAKT signaling remains unaltered. (*A*) Representative composite Western illustrating decreased pERK levels in mutant microdissected heart/cardiac ganglia (*) compared with wild type at both E14.5 and P7 but equivalent total ERK levels ($n = 5$). However, cKO pAKT levels were unaltered at these ages ($n = 3$). (*B*) Densitometry quantification of pERK to tERK ratios at E14.5 and P7 [*t* test, *P value < 0.05 (E14.5, P value = 0.0052; P7, P value = 0.0008)]. (*C*) Densitometry quantification of pAKT to tAKT ratios [*t* test, P value = 0.498 (E14.5); P value = 0.758 (P7)]. Error bars represent SEM. The significant reduction in pERK levels suggests that a disproportionate amount of the active pERK signaling in our neonatal microdissected heart/cardiac ganglia samples was within the NC/*Postn-Cre*-positive lineage. Moreover, unlike both total ERK1,2 and SHP-2, which are ubiquitously expressed, pERK levels are known to fluctuate within a dynamic spatiotemporal tissue-restricted pattern in both mouse (88) and human tissues (89).

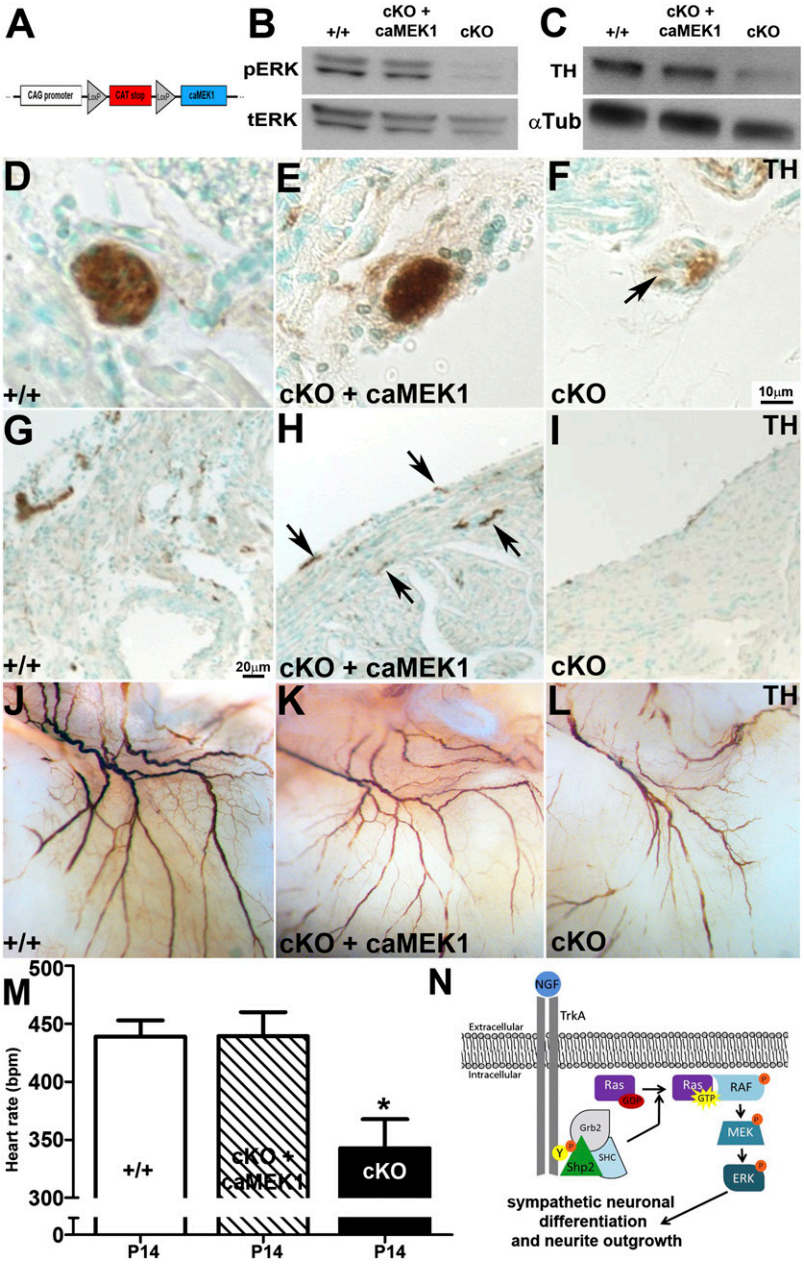

Fig. 5. Lineage-specific expression of caMEK1 rescues the sympathetic innervation phenotype of *Shp2* cKOs. (*A*) Schematic of *caMEK1* genetic construct. (*B*) Western analysis of heart isolates demonstrated that pERK levels in a rescued mutant (cKO + caMEK1) are similar to those in wild-type littermates, whereas pERK in a cKO mutant is still drastically decreased. (*C*) Western analysis of heart isolates demonstrated that TH levels are also normalized in a rescued mutant and are similar to a wild-type littermate, but TH levels relative to α-tubulin loading control are still drastically decreased in cKO hearts. (*D–F*) TH IHC of P14 control (*D*), rescue (*E*), and mutant (arrow in *F*) cardiac ganglia demonstrating a restoration of TH expression in the rescued mutant ganglia. (*G–I*) TH IHC of P14 control (*G*), rescue (*H*), and mutant (*I*) left ventricle demonstrating increased TH-positive innervation in the rescued mutant ventricle (arrows in *H*). (Scale bar: 20 μm.) (*J–L*) Whole mount TH IHC showing the dorsal surface pattern of sympathetic innervation in a P14 control (*J*), rescued mutant (*K*), and mutant (*L*) heart. (*M*) ECG analysis of average heart rates of control, rescue, and mutant littermates at P14 [one-way ANOVA $P = 0.0113$; Tukey's multiple comparisons test: $^{+/+}$ vs. rescue = nonsignificant, $^{+/+}$ vs. cKO = significant ($P < 0.05$), rescue vs. cKO = significant ($P < 0.05$) $n = 5–20$]. Note that lineage-specific expression of caMEK1 restores the mutant heart rates. (*N*) Proposed model for underlying signaling cascade responsible for the sympathetic innervation defects within *Shp2* cKOs. Error bars represent SEM.

elevated the heart rates of the rescued mutants to those of littermate controls. One aspect of the genetic intercross was that mixing the *SHP-2* cKO model (on a predominantly C57BL/6 background) with the *caMEK1* model (on a pure FVB/N background) equivalently shifted the basal heart rates of both control and mutant littermates ([C57BL/6 control, 499.77 ± 10.25 beats per minute (bpm); mixed background control, 439.00 ± 14.00 bpm; C57BL/6 *Shp2* cKO, 383.51 ± 5.26 bpm; mixed background *Shp2* cKO, 342.83 ± 25.00 bpm; $n = 6–20$]. This is not surprising, because different backgrounds can have widely divergent basal heart rates (76). Because this shift affected all genotypes to the same extent and the relationship between control and *Shp2* cKO heart rates was not altered, it was not investigated further and was instead considered evidence that the mechanism for cardiac sympathetic innervation described in this study holds true on more than one genetic background. Based on the neurite

outgrowth studies, innervation phenotypes, pERK-dependent rescue, and previous in vitro work, we propose a schematic detailing the likely signaling mechanism as explanation for these data (Fig. 5*N*).

Discussion

In this study we explored the role of SHP-2 and downstream pERK signaling in the context of sympathetic neuron differentiation and innervation maintenance of the developing heart. Although much is known about the molecular mechanisms regulating sympathetic neuron growth and differentiation in vitro, many of these pathways had yet to be investigated in vivo. We generated a lineage specific KO of *Shp2*, which exhibits postnatal failure of sympathetic cardiac innervation. Furthermore, the fact that restoration of pERK levels rescued this phenotype indicates that pERK signaling is necessary for peripheral sympathetic innervation in vivo. SHP-2 has been shown in vitro to be a required intermediary linking NGF signaling to pERK elevation, which is essential for sympathetic neuron differentiation (57–59, 77–81). When the NGF–SHP-2–ERK pathway is interrupted in model systems such as PC12 cells and explanted superior cervical ganglia via pharmacological or genetic means, sympathetic neurons fail to differentiate (as indicated by the paucity of neurites projected from the cell body) (57–59, 77–81). Although some in vivo models have indicated an important role for MAPK signaling in sensory innervation patterning (41), other groups have attempted to investigate the effect of SHP-2 mutations on sympathetic innervation in vivo but were unable to recapitulate the in vitro results (77); our *Shp2* cKO successfully demonstrates that SHP-2 and subsequent pERK elevation are required for sympathetic innervation of the developing heart. Although the *Postn-Cre* is expressed from E10.5 onward, phenotypic differences between cKOs and controls were not observed until after birth. This could be due to the fact that NGF and its downstream signaling are not required for sympathetic innervation until E16.5 (82), but in the absence of an inducible Cre we cannot exclude the possibility that NC progenitors are altered or misspecified early in development and the effects are not manifested until after birth. This is a limitation of the current study and is an avenue of future research when the appropriate genetic tools become available.

Although global cardiac sympathetic innervation was diminished in cKOs, the TH-positive intrinsic cardiac ganglia exhibited decreased neurite outgrowth and TH expression. This emphasizes that these structures are subject to the influences of SHP-2 and pERK signaling and, in the context of sinus bradycardia, reinforces their functional role in the heart brain and the idea that they are involved in heart rate regulation particularly in the first 2–3 wk of life (22, 23, 25, 26). The dearth of axonal projections emanating from these ganglia combined with the loss of sympathetic-specific TH expression despite continued expression of the generic neuronal marker NSβT suggests that failure of sympathetic neurons to differentiate or to maintain their differentiated state may be the underlying mechanism for the altered sympathetic innervation in mutant hearts. Aberrant expression of embryonic sympathetic neuron differentiation transcription factors such as *Phox2a* and *2b* which regulate TH and Dopamine β-hydroxylase expression (11) further supports this hypothesis. Additionally, the absence of apoptotic cells in mutant sympathetic ganglia emphasizes the fact that MAPK signaling is essential for differentiation but not for the survival of sympathetic neurons. Thus, although these SHP-2–regulated protein kinases have pleotropic effects on the cell, they likely elicit some of their effects by the phosphorylation of downstream mediators of sympathetic nervous system homeostatic gene expression.

MEK1 is an ideal target for a genetic rescue of our model because the only known substrates of MEKs are ERK1/2, and reciprocally, the only known activators of ERK1/2 are MEK1/2 (58). Although both MEK1 and 2 are known to activate ERK, MEK1 has been more extensively studied and is considered the more physiologically relevant isoform particularly downstream of RAS because MEK1 but not MEK2 has been found to associate with RAS in a signaling complex (83). Specifically, in PC12 cells an inactivating mutation in MEK1 blocks sympathetic differentiation, whereas activating mutations facilitate neurite outgrowth even in the presence of dominant-negative SHP-2 or in the absence of NGF (57, 59). Introduction of caMEK driven by the same conditional system as our *Shp2* cKO allowed us to simultaneously delete SHP-2 and express caMEK in postmigratory NC. Significantly, this model resulted in a physiological increase in pERK levels (restored to control levels) because unchecked elevation of pERK can result in cardiac valvular and septal abnormalities (84). The spatiotemporal precision of this genetic model has allowed us to begin to parse out the ERK-dependent from the ERK-independent effects of *Shp2* cKO. The rescued mutants (*Shp2;Postn-Cre;caMEK*) still exhibit failure to thrive and eventually die, although a significant portion (~50%) survive past weaning, whereas all nonrescued mutants die before P21. The delay but not complete rescue of lethality indicates that there may be both ERK-dependent and ERK-independent mechanisms contributing to the eventual death of the mice. For example, the peripheral innervation defects and altered enteric innervation, although not the focus of this study, could be contributing factors to lethality in both the cKO and rescued model (*SI Appendix*). An alternative explanation is that there is not complete rescue due to the fact that dynamic pERK regulation cannot be achieved through constitutive expression of caMEK1. Significantly, our findings indicate that establishment of sympathetic innervation of the heart is an ERK-dependent event because all aspects of the cardiac innervation phenotype observed in the *Shp2* cKO were rescued by lineage-restricted caMEK1. This model provides a useful tool in which to identify lineage-specific proximate targets of SHP-2 during autonomic innervation and establishment of a mature functioning cardiovascular system.

Functionally, we have demonstrated that SHP-2–dependent sympathetic deficiency leads to sinus bradycardia. Because there is diminished sympathetic innervation in the mutant heart and the innervation which is present lacks TH and thus cannot produce catecholamines (i.e., norepinephrine) which would normally act to maintain the heart rate, we hypothesized that delivering an exogenous β-adrenergic agonist (isoproterenol) would stimulate both the control and the mutant heart to beat faster. Because isoproterenol did increase both the control and the mutant heart rates equivalently, we were able to conclude that the mutant heart is functionally capable of responding to catecholamines and maintaining a rapid heart rate (excluding the possibility of conduction or inherent structural defects as a cause of the bradycardia). Furthermore, because administration of atropine did not elevate heart rate, indicating that parasympathetic tone is not responsible for the slowed heart rate, we concluded that the absence of sympathetic tone is the direct cause of the sinus bradycardia observed in *Shp2* cKOs. This hypothesis was further verified by rescuing the sympathetic innervation phenotype by conditionally expressing caMEK1 which abolished the sinus bradycardia. Through lending mechanistic insight to early sympathetic innervation and heart rate regulation, this model also allows for investigation of how the loss of SHP-2 function in diseases such as LEOPARD syndrome can lead to the ECG abnormalities characteristic of the syndrome (47, 51). Although these abnormalities are not very well characterized and are often complicated by structural cardiac defects and a uniform decrease of SHP-2 signaling within all tissues at all ages (51, 85–87), our cKO mouse provides an opportunity to study SHP-2's spatiotemporal role in establishing aberrant ECG patterning in isolation from compounding structural cardiac defects.

Materials and Methods

Animal use was in accordance with institutional guidelines, and all experiments were reviewed and approved by the Institutional Animal Care and Use Committee at Indiana University-Purdue University Indianapolis. Floxed *Shp2* mice were generated as described previously (50) and intercrossed with *Postn-Cre* [MGI:3775923] mice on a C57BL/6 background to generate lineage-restricted cKO offspring (60) containing a 3.9 kb partial *Periostin* promoter that drives Cre expression within the NC-derived peripheral nervous system (including Schwann cells as well as sensory, enteric, and sympathetic neurons) (62). To facilitate lineage mapping, floxed *Shp2;Postn-Cre* mice were intercrossed with β-galactosidase indicator mice (61). To reconstitute pERK expression within the *Shp2* cKO lineage, the floxed *Shp2;Postn-Cre* mice were intercrossed with *CAG-caMEK1* mice (75) which were on a pure FVB/N background. The resulting ♂*CAG-caMEK1;Postn-Cre;Shp2*$^{f/+}$ mice were bred to existing ♀*Shp2*$^{f/f}$*;R26r/R26r* mice which yielded our desired compound mutant experimental genotype: *CAG-MEK1;Postn-Cre;Shp2*$^{f/f}$*;R26r* ~3/16 pups born.

Additional methods are detailed in *SI Appendix*.

ACKNOWLEDGMENTS. These studies were supported, in part, by American Heart Association Predoctoral Grant 13PRE16920038 (to J.D.L.), the Riley Children's Foundation, Indiana University Department of Pediatrics (Neonatal-Perinatal Medicine), and National Institutes of Health Grant R01HL60714 (to S.J.C.).

1. Ieda M, Fukuda K (2009) Cardiac innervation and sudden cardiac death. *Curr Cardiol Rev* 5(4):289–295.
2. Cao JM, et al. (2000) Nerve sprouting and sudden cardiac death. *Circ Res* 86(7): 816–821.
3. Packer M (1992) The neurohormonal hypothesis: A theory to explain the mechanism of disease progression in heart failure. *J Am Coll Cardiol* 20(1):248–254.
4. Verrier RL, Antzelevitch C (2004) Autonomic aspects of arrhythmogenesis: The enduring and the new. *Curr Opin Cardiol* 19(1):2–11.
5. Huber K (2006) The sympathoadrenal cell lineage: Specification, diversification, and new perspectives. *Dev Biol* 298(2):335–343.
6. Loring JF, Erickson CA (1987) Neural crest cell migratory pathways in the trunk of the chick embryo. *Dev Biol* 121(1):220–236.
7. Guillemot F, et al. (1993) Mammalian achaete-scute homolog 1 is required for the early development of olfactory and autonomic neurons. *Cell* 75(3):463–476.
8. Howard MJ, Stanke M, Schneider C, Wu X, Rohrer H (2000) The transcription factor dHAND is a downstream effector of BMPs in sympathetic neuron specification. *Development* 127(18):4073–4081.
9. Pattyn A, Morin X, Cremer H, Goridis C, Brunet JF (1999) The homeobox gene Phox2b is essential for the development of autonomic neural crest derivatives. *Nature* 399(6734):366–370.
10. Lim KC, et al. (2000) Gata3 loss leads to embryonic lethality due to noradrenaline deficiency of the sympathetic nervous system. *Nat Genet* 25(2):209–212.
11. Stanke M, et al. (1999) The Phox2 homeodomain proteins are sufficient to promote the development of sympathetic neurons. *Development* 126(18):4087–4094.
12. Morin X, et al. (1997) Defects in sensory and autonomic ganglia and absence of locus coeruleus in mice deficient for the homeobox gene Phox2a. *Neuron* 18(3):411–423.
13. Coppola E, d'Autréaux F, Rijli FM, Brunet JF (2010) Ongoing roles of Phox2 homeodomain transcription factors during neuronal differentiation. *Development* 137(24): 4211–4220.
14. Cochard P, Goldstein M, Black IB (1978) Ontogenetic appearance and disappearance of tyrosine hydroxylase and catecholamines in the rat embryo. *Proc Natl Acad Sci USA* 75(6):2986–2990.
15. Ernsberger U, et al. (1995) The expression of tyrosine hydroxylase and the transcription factors cPhox-2 and Cash-1: Evidence for distinct inductive steps in the differentiation of chick sympathetic precursor cells. *Mech Dev* 52(1):125–136.
16. Ernsberger U (2009) Role of neurotrophin signalling in the differentiation of neurons from dorsal root ganglia and sympathetic ganglia. *Cell Tissue Res* 336(3):349–384.
17. Cochard P, Paulin D (1984) Initial expression of neurofilaments and vimentin in the central and peripheral nervous system of the mouse embryo in vivo. *J Neurosci* 4(8): 2080–2094.
18. Groves AK, et al. (1995) Differential regulation of transcription factor gene expression and phenotypic markers in developing sympathetic neurons. *Development* 121(3): 887–901.
19. Schneider C, Wicht H, Enderich J, Wegner M, Rohrer H (1999) Bone morphogenetic proteins are required in vivo for the generation of sympathetic neurons. *Neuron* 24(4):861–870.
20. Rysevaite K, et al. (2011) Morphologic pattern of the intrinsic ganglionated nerve plexus in mouse heart. *Heart Rhythm* 8(3):448–454.
21. Rysevaite K, et al. (2011) Immunohistochemical characterization of the intrinsic cardiac neural plexus in whole-mount mouse heart preparations. *Heart Rhythm* 8(5): 731–738.
22. Kukanova B, Mravec B (2006) Complex intracardiac nervous system. *Bratisl Lek Listy (Tlacene Vyd)* 107(3):45–51.
23. Horackova M, Slavikova J, Byczko Z (2000) Postnatal development of the rat intrinsic cardiac nervous system: A confocal laser scanning microscopy study in whole-mount atria. *Tissue Cell* 32(5):377–388.
24. Habecker BA, et al. (2008) Regulation of cardiac innervation and function via the p75 neurotrophin receptor. *Auton Neurosci* 140(1–2):40–48.
25. Huang MH, et al. (1996) An intrinsic adrenergic system in mammalian heart. *J Clin Invest* 98(6):1298–1303.
26. Hoard JL, et al. (2008) Cholinergic neurons of mouse intrinsic cardiac ganglia contain noradrenergic enzymes, norepinephrine transporters, and the neurotrophin receptors tropomyosin-related kinase A and p75. *Neuroscience* 156(1):129–142.
27. Shoba T, Tay SS (2000) Nitrergic and peptidergic innervation in the developing rat heart. *Anat Embryol (Berl)* 201(6):491–500.
28. Rimmer K, Harper AA (2006) Developmental changes in electrophysiological properties and synaptic transmission in rat intracardiac ganglion neurons. *J Neurophysiol* 95(6):3543–3552.
29. Robinson RB (1996) Autonomic receptor—effector coupling during post-natal development. *Cardiovasc Res* 31(Spec No):E68–E76.
30. De Champlain J, Malmfors T, Olson L, Sachs C (1970) Ontogenesis of peripheral adrenergic neurons in the rat: Pre- and postnatal observations. *Acta Physiol Scand* 80(2): 276–288.
31. Saygili E, et al. (2012) Age-related regional differences in cardiac nerve growth factor expression. *Age (Dordr)* 34(3):659–667.
32. Klesse LJ, Meyers KA, Marshall CJ, Parada LF (1999) Nerve growth factor induces survival and differentiation through two distinct signaling cascades in PC12 cells. *Oncogene* 18(12):2055–2068.
33. Virdee K, Tolkovsky AM (1995) Activation of p44 and p42 MAP kinases is not essential for the survival of rat sympathetic neurons. *Eur J Neurosci* 7(10):2159–2169.
34. Virdee K, Tolkovsky AM (1996) Inhibition of p42 and p44 mitogen-activated protein kinase activity by PD98059 does not suppress nerve growth factor-induced survival of sympathetic neurones. *J Neurochem* 67(5):1801–1805.
35. Snider WD (1994) Functions of the neurotrophins during nervous system development: What the knockouts are teaching us. *Cell* 77(5):627–638.
36. Smeyne RJ, et al. (1994) Severe sensory and sympathetic neuropathies in mice carrying a disrupted Trk/NGF receptor gene. *Nature* 368(6468):246–249.
37. Ruit KG, Snider WD (1991) Administration or deprivation of nerve growth factor during development permanently alters neuronal geometry. *J Comp Neurol* 314(1): 106–113.
38. Crowley C, et al. (1994) Mice lacking nerve growth factor display perinatal loss of sensory and sympathetic neurons yet develop basal forebrain cholinergic neurons. *Cell* 76(6):1001–1011.
39. Ieda M, et al. (2007) Sema3a maintains normal heart rhythm through sympathetic innervation patterning. *Nat Med* 13(5):604–612.
40. Maden CH, et al. (2012) NRP1 and NRP2 cooperate to regulate gangliogenesis, axon guidance and target innervation in the sympathetic nervous system. *Dev Biol* 369(2): 277–285.
41. Newbern JM, et al. (2011) Specific functions for ERK/MAPK signaling during PNS development. *Neuron* 69(1):91–105.
42. Edouard T, et al. (2007) How do Shp2 mutations that oppositely influence its biochemical activity result in syndromes with overlapping symptoms? *Cell Mol Life Sci* 64(13):1585–1590.
43. Stewart RA, et al. (2010) Phosphatase-dependent and -independent functions of Shp2 in neural crest cells underlie LEOPARD syndrome pathogenesis. *Dev Cell* 18(5): 750–762.
44. Grossmann KS, Rosário M, Birchmeier C, Birchmeier W (2010) The tyrosine phosphatase Shp2 in development and cancer. *Adv Cancer Res* 106:53–89.
45. Qu CK (2000) The SHP-2 tyrosine phosphatase: signaling mechanisms and biological functions. *Cell Res* 10(4):279–288.
46. Tidyman WE, Rauen KA (2009) The RASopathies: Developmental syndromes of Ras/MAPK pathway dysregulation. *Curr Opin Genet Dev* 19(3):230–236.
47. Kontaridis MI, Swanson KD, David FS, Barford D, Neel BG (2006) PTPN11 (Shp2) mutations in LEOPARD syndrome have dominant negative, not activating, effects. *J Biol Chem* 281(10):6785–6792.
48. Tartaglia M, et al. (2006) Diversity and functional consequences of germline and somatic PTPN11 mutations in human disease. *Am J Hum Genet* 78(2):279–290.
49. Neel BG, Gu H, Pao L (2003) The 'Shp'ing news: SH2 domain-containing tyrosine phosphatases in cell signaling. *Trends Biochem Sci* 28(6):284–293.
50. Zhang EE, Chapeau E, Hagihara K, Feng GS (2004) Neuronal Shp2 tyrosine phosphatase controls energy balance and metabolism. *Proc Natl Acad Sci USA* 101(45): 16064–16069.
51. Torres J, Russo P, Tobias JD (2004) Anaesthetic implications of LEOPARD syndrome. *Paediatr Anaesth* 14(4):352–356.
52. Tartaglia M, Zampino G, Gelb BD (2010) Noonan syndrome: clinical aspects and molecular pathogenesis. *Mol Syndromol* 1(1):2–26.
53. Nakamura T, Gulick J, Colbert MC, Robbins J (2009) Protein tyrosine phosphatase activity in the neural crest is essential for normal heart and skull development. *Proc Natl Acad Sci USA* 106(27):11270–11275.
54. Saxton TM, Pawson T (1999) Morphogenetic movements at gastrulation require the SH2 tyrosine phosphatase Shp2. *Proc Natl Acad Sci USA* 96(7):3790–3795.
55. Chen B, et al. (2000) Mice mutant for Egfr and Shp2 have defective cardiac semilunar valvulogenesis. *Nat Genet* 24(3):296–299.
56. Grossmann KS, et al. (2009) The tyrosine phosphatase Shp2 (PTPN11) directs Neuregulin-1/ErbB signaling throughout Schwann cell development. *Proc Natl Acad Sci USA* 106(39):16704–16709.

57. Marshall CJ (1995) Specificity of receptor tyrosine kinase signaling: Transient versus sustained extracellular signal-regulated kinase activation. *Cell* 80(2):179–185.
58. Cowley S, Paterson H, Kemp P, Marshall CJ (1994) Activation of MAP kinase kinase is necessary and sufficient for PC12 differentiation and for transformation of NIH 3T3 cells. *Cell* 77(6):841–852.
59. Wright JH, et al. (1997) A role for the SHP-2 tyrosine phosphatase in nerve growth-induced PC12 cell differentiation. *Mol Biol Cell* 8(8):1575–1585.
60. Joseph NM, et al. (2008) The loss of Nf1 transiently promotes self-renewal but not tumorigenesis by neural crest stem cells. *Cancer Cell* 13(2):129–140.
61. Soriano P (1999) Generalized lacZ expression with the ROSA26 Cre reporter strain. *Nat Genet* 21(1):70–71.
62. Lindsley A, et al. (2007) Identification and characterization of a novel Schwann and outflow tract endocardial cushion lineage-restricted periostin enhancer. *Dev Biol* 307(2):340–355.
63. Takeda N, et al. (2010) Cardiac fibroblasts are essential for the adaptive response of the murine heart to pressure overload. *J Clin Invest* 120(1):254–265.
64. Lajiness JD, Conway SJ (2012) The dynamic role of cardiac fibroblasts in development and disease. *J Cardiovasc Transl Res* 5(6):739–748.
65. Ke Y, et al. (2007) Deletion of Shp2 in the brain leads to defective proliferation and differentiation in neural stem cells and early postnatal lethality. *Mol Cell Biol* 27(19): 6706–6717.
66. Chuma S, Nakatsuji N (2001) Autonomous transition into meiosis of mouse fetal germ cells in vitro and its inhibition by gp130-mediated signaling. *Dev Biol* 229(2):468–479.
67. Hohimer AR, Davis LE, Hatton DC (2005) Repeated daily injections and osmotic pump infusion of isoproterenol cause similar increases in cardiac mass but have different effects on blood pressure. *Can J Physiol Pharmacol* 83(2):191–197.
68. Shusterman V, et al. (2002) Strain-specific patterns of autonomic nervous system activity and heart failure susceptibility in mice. *Am J Physiol Heart Circ Physiol* 282(6): H2076–H2083.
69. Saba S, London B, Ganz L (2003) Autonomic blockade unmasks maturational differences in rate-dependent atrioventricular nodal conduction and facilitation in the mouse. *J Cardiovasc Electrophysiol* 14(2):191–195.
70. Clegg DO, Large TH, Bodary SC, Reichardt LF (1989) Regulation of nerve growth factor mRNA levels in developing rat heart ventricle is not altered by sympathectomy. *Dev Biol* 134(1):30–37.
71. Chan G, et al. (2011) Essential role for Ptpn11 in survival of hematopoietic stem and progenitor cells. *Blood* 117(16):4253–4261.
72. Schramm C, Fine DM, Edwards MA, Reeb AN, Krenz M (2012) The PTPN11 loss-of-function mutation Q510E-Shp2 causes hypertrophic cardiomyopathy by dysregulating mTOR signaling. *Am J Physiol Heart Circ Physiol* 302(1):H231–H243.
73. Marin TM, et al. (2011) Rapamycin reverses hypertrophic cardiomyopathy in a mouse model of LEOPARD syndrome-associated PTPN11 mutation. *J Clin Invest* 121(3): 1026–1043.
74. Ishida H, et al. (2011) LEOPARD-type SHP2 mutant Gln510Glu attenuates cardiomyocyte differentiation and promotes cardiac hypertrophy via dysregulation of Akt/GSK-3β/β-catenin signaling. *Am J Physiol Heart Circ Physiol* 301(4):H1531–H1539.
75. Krenz M, et al. (2008) Role of ERK1/2 signaling in congenital valve malformations in Noonan syndrome. *Proc Natl Acad Sci USA* 105(48):18930–18935.
76. Hoit BD, et al. (2002) Naturally occurring variation in cardiovascular traits among inbred mouse strains. *Genomics* 79(5):679–685.
77. Chen B, Hammonds-Odie L, Perron J, Masters BA, Bixby JL (2002) SHP-2 mediates target-regulated axonal termination and NGF-dependent neurite growth in sympathetic neurons. *Dev Biol* 252(2):170–187.
78. Rosário M, Franke R, Bednarski C, Birchmeier W (2007) The neurite outgrowth multiadaptor RhoGAP, NOMA-GAP, regulates neurite extension through SHP2 and Cdc42. *J Cell Biol* 178(3):503–516.
79. Kaplan DR, Miller FD (2000) Neurotrophin signal transduction in the nervous system. *Curr Opin Neurobiol* 10(3):381–391.
80. Gill JS, Schenone AE, Podratz JL, Windebank AJ (1998) Autocrine regulation of neurite outgrowth from PC12 cells by nerve growth factor. *Brain Res Mol Brain Res* 57(1): 123–131.
81. Grewal SS, York RD, Stork PJ (1999) Extracellular-signal-regulated kinase signalling in neurons. *Curr Opin Neurobiol* 9(5):544–553.
82. Ieda M, et al. (2004) Endothelin-1 regulates cardiac sympathetic innervation in the rodent heart by controlling nerve growth factor expression. *J Clin Invest* 113(6): 876–884.
83. Jelinek T, et al. (1994) RAS and RAF-1 form a signalling complex with MEK-1 but not MEK-2. *Mol Cell Biol* 14(12):8212–8218.
84. Araki T, et al. (2009) Noonan syndrome cardiac defects are caused by PTPN11 acting in endocardium to enhance endocardial-mesenchymal transformation. *Proc Natl Acad Sci USA* 106(12):4736–4741.
85. Smith RF, Pulicicchio LU, Holmes AV (1970) Generalized lentigo: Electrocardiographic abnormalities, conduction disorders and arrhythmias in three cases. *Am J Cardiol* 25(4):501–506.
86. Woywodt A, et al. (1998) Cardiomyopathic lentiginosis/LEOPARD syndrome presenting as sudden cardiac arrest. *Chest* 113(5):1415–1417.
87. Limongelli G, et al. (2008) Genotype-phenotype analysis and natural history of left ventricular hypertrophy in LEOPARD syndrome. *Am J Med Genet A* 146A(5):620–628.
88. Corson LB, Yamanaka Y, Lai KM, Rossant J (2003) Spatial and temporal patterns of ERK signaling during mouse embryogenesis. *Development* 130(19):4527–4537.
89. Rouleau C, Matécki S, Kalfa N, Costes V, de Santa Barbara P (2009) Activation of MAP kinase (ERK1/2) in human neonatal colonic enteric nervous system. *Neurogastroenterol Motil* 21(2):207–214.